



Virtual Captive Model tests for Maneuvering Prediction

Obaid Ullah Khan¹, Asif Mansoor¹, Behzad Ahmed Zai¹, Najam us Saqib^{2,*}, Murtza Hussain¹, Tariq Jamil²

ARTICLE INFO

Article history:

Received 25 Oct 2022;
in revised from 25 Oct 2022;
accepted 31 Oct 2022.

Keywords:

CFD, Maneuvering, Hydrodynamic derivatives, STARCCM+, Planner motion mechanism.

ABSTRACT

Maneuvering in general is the ability of the ship to follow the desired path with the help of its control surfaces, it cannot be put into a quantifiable term. This paper uses commercial CFD software “Simcenter STARCCM+” for performing virtual captive model tests. A benchmark KCS Hull has been adopted for this study. Test conditions of PMM tests from the SIMMAN 2008 workshop have been replicated in the virtual captive model tests. Static as well as dynamic tests have been performed to determine the hydrodynamic derivatives and have been validated against the experimental values. These derivatives are then used to determine the directional straight-line stability of the ship. The results showed that the simulated values of the derivatives match well with the experimental values. This paper also presents the ability of STARCCM+ software in predicting the maneuvering characteristics of the ship with its advanced built-in Planner motion mechanism, general motion mechanism, and rotating arm tests. The use of dynamic fluid body interaction with planner motion mechanism has been presented in this paper.

© SEECMAR | All rights reserved

1. Introduction.

Ship course stability and turning ability check are of great importance during the initial design stage. These abilities are evaluated using the hydrodynamic maneuvering characteristics of the ship. Captive model tests are used to determine the hydrodynamic derivatives in both static and dynamic conditions of the ship. However, model tests have some limitations, such as cost and time, because the design is frequently changed in the initial stages. Therefore many simulation-based methods are used to determine ship maneuvering performance. The Maneuvering committee of the 24th international towing tank Conference (ITTC)[[1] categorizes maneuvering simulations into three groups: No simulation, system-based simulation, and computational methods. No simulation method contains the database to determine hydrodynamic coefficients, system-based methods are model testing based captive model tests and the computational methods involve virtual captive model tests. The ad-

vancements in the computational methods have implemented CFD-based simulations in finding ship maneuverability [2]. CFD-based methods are additionally divided into two groups for accessing the maneuverability of a ship i.e the direct maneuvering method and the indirect maneuvering method.

The direct maneuvering method involves the resolution of propeller and rudder to predict the motion of the ship [3], it is the best known hydrodynamic model and it can simulate any maneuvering including many additional effects such as sloshing, wind waves, etc. Besides the motion response, extensive data of the flow field is available like pressure distribution, flow field, waves, segmented forces, rudder forces, and rudder-propeller Hull interaction. It is not suitable for exploring huge design space due to the high computational requirement as a very small time step for propeller modeling makes the simulation expensive.

Indirect maneuvering simulations find the hydrodynamic coefficients in a fast and efficient way using the inbuilt Planner motion mechanism in STARCCM+. Arbitrary rudder maneuvers are then possible for one operational point using the obtained hydrodynamic coefficients from the virtual captive model tests and the mathematical model. Abkowitz mathematical model [4] is used in this study.

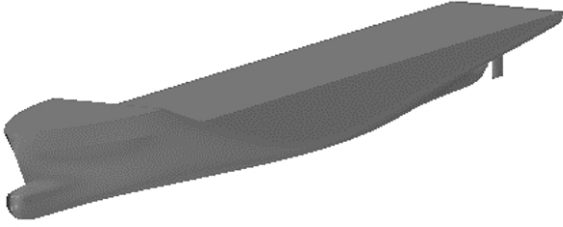
CFD has shown many promising results thus more and more people are using CFD for predicting final maneuvers. The SIM-

¹Department of Engineering Sciences, PN Engineering College, National University of Sciences and Technology (NUST), Karachi, Pakistan.

²Department of Mechanical Engineering, NED University, Karachi, Pakistan.

*Corresponding author: Najam us Saqib. E-mail Address: najamus-saqib1987@gmail.com.

Figure 1: KCS Hull container ship.



Source: Authors.

MAN [5-6] workshop on Maneuvering prediction uses the captive model testing approach to determine hydrodynamic coefficients using PMM data, only a few cases showed the final maneuvers. Much work has been done on the individual PMM tests for instance static and dynamic PMM tests were computed for the kvcc12 to determine hydrodynamic derivatives [7], same tests were computed for DTMB 5415 surface combatant to determine the derivatives [8]. This paper presents the course stability check and validation of hydrodynamic derivatives of a benchmark KCS hull. It also presents the ability of a commercial CFD software STARCCM+ in predicting ships maneuvering characteristics.

2. Geometry of Ship.

The hull form and the geometric characteristic of the hull were obtained from the SIMMAN website [5]. The ship is a container ship with a bulbous bow, transom stern, and appended with rudder and propeller. The original length of the ship is 230m and it was scaled by a factor of 52.667, the model scale length between perpendiculars is 4.367m and the draught is 0.20506m. The design speed of the ship is 24 knots. Fig 1 shows the hull form of the ship with the rudder attached to it. The Hull form characteristics and other dimensional parameters are given in Table 1.

Table 1: Dimensional Parameters of KCS Hull.

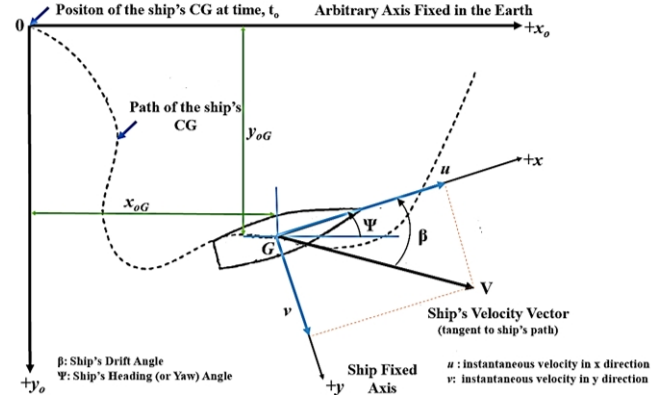
Component	Main Variables	Full scale	Model scale	Unit
Hull	Length between perpendiculars (L _{pp})	230	4.3671	m
	Load waterline length (L _{wl})	232.5	4.4141	m
	Beam waterline length (B _{wl})	32.2	0.6114	m
	Depth (D)	19	0.450	m
	Draught (T)	10.8	0.2051	m
	Displacement (V)	52030	0.3562	m ³
	Surface w/o rudder (S)	9530	3.4357	m ²
	Block coefficient (CB)	0.651	0.651	-
Rudder	Midship coefficient (CM)	0.985	0.984	-
	Surface area of rudder	115	0.0415	m ²
Propeller	Lateral Area of rudder	54.45	0.0196	m ²
	Turn rate	2.32	16.8	Deg/s
	No of blades	05	05	-
	Diameter (D)	7.9	0.150	m
	Rotation	Right handed	Right handed	-
Propeller	Hub ratio	0.180	0.227	-
	P/D	0.997	1.30	-

Source: Authors.

According to the standard maneuvering coordinate system shown in Fig 2. Two coordinate systems were chosen, the body-fixed coordinate system and the earth fixed coordinate system.

X is positive in the surge direction and y is positive in the starboard direction. It is located at the center of gravity point of the ship. Earth fixed coordinate system was made at the intersection of the free surface and the centerline of the ship. The rudder angle is positive when rotated towards the port side and vice versa. The drift angle is positive when rotated towards the starboard side and vice versa.

Figure 2: Standard maneuvering coordinate system (PNA III).



Source: Authors.

3. Mathematical model.

There are many mathematical models to describe the forces and moments acting on the ship, the most commonly used models are the Mathematical modeling group (MMG) [9] and the Abkowitz model. The main difference between these two models is that the Abkowitz model models the hull rudder propeller interaction whereas in MMG the hydrodynamic forces acting on the hull rudder and the propeller are modeled individually, so the Abkowitz model is preferred in this study. In maneuvering for a surface ship moving in calm and deep water, it is assumed that the roll, heave, and pitch is negligible so the 6DOF equations of motion reduce to 3DOF equations i.e surge, sway, and yaw. The Abkowitz model for the 3 DOF maneuvering equations are

$$m(\dot{u} - rv - x_G \dot{r}^2) = X$$

$$m(\dot{v} + ur - x_G \dot{r}) = Y$$

$$I_Z \dot{r} + mx_G(\dot{v} + ur) = N$$

Where X and Y are the surges and sway forces, N is the Yaw moment. I_z is the moment of inertia around the z-axis, x_G is the longitudinal distance of the center of gravity, u v and r are the surges, sway, and yaw velocities and \dot{u} , \dot{v} , \dot{r} are the corresponding accelerations and m is the mass of the ship. In the Abkowitz model, the hydrodynamic forces on a ship are expressed as a polynomial function of the maneuvering parameter and the control parameters i.e. the propeller revolution, and rudder angle, in the form of the Tylor series. The expansion of this Taylor series [10] leads to the following equations for X Y and N.

$$X = X_* + X_{\dot{u}}\dot{u} + X_u\Delta u + X_{uu}\Delta u^2 + X_{uuu}\Delta u^3 + X_{vv}v^2 + X_{rr}r^2 + X_{\delta\delta}\delta^2 + X_{v\dot{v}}v\dot{v} + X_{vu}v\Delta u + X_{vuu}v\Delta u^2 + X_{\delta\delta\delta}\delta^3 + X_{vr}vr + X_{v\delta}v\delta + X_{r\delta}r\delta + X_{vru}vr\Delta u + X_{v\delta u}v\delta\Delta u + X_{r\delta u}r\delta\Delta u$$

$$Y = Y_* + Y_u\Delta u + Y_{uu}\Delta u^2 + Y_{uuu}\Delta u^3 + Y_{\dot{v}}\dot{v} + Y_vv + Y_{vv}v^2 + Y_{vrr}vr^2 + Y_{v\delta\delta}v\delta^2 + Y_{vu}v\Delta u + Y_{vuu}v\Delta u^2 + Y_{\dot{r}}\dot{r} + Y_r r + Y_{rr}r^2 + Y_{rv}rv + Y_{r\delta}r\delta + Y_{ru}r\Delta u + Y_{ruu}r\Delta u^2 + Y_{\delta}\delta + Y_{\delta\delta\delta}\delta^3 + Y_{\delta v}\delta v^2 + X_{\delta rr}\delta r^2 + Y_{\delta u}\delta\Delta u + Y_{\delta uu}\delta\Delta u^2 + Y_{\delta\delta\delta u}\delta^3\Delta u + Y_{v\delta}vr\delta$$

$$N = N_* + N_u\Delta u + N_{uu}\Delta u^2 + N_{uuu}\Delta u^3 + N_{\dot{v}}\dot{v} + N_vv + N_{vv}v^2 + N_{vrr}vr^2 + N_{v\delta\delta}v\delta^2 + N_{vu}v\Delta u + N_{vuu}v\Delta u^2 + N_{\dot{r}}\dot{r} + N_r r + N_{rr}r^2 + N_{rv}rv + N_{r\delta}r\delta + N_{ru}r\Delta u + N_{ruu}r\Delta u^2 + N_{\delta}\delta + N_{\delta\delta\delta}\delta^3 + N_{\delta v}\delta v^2 + N_{\delta rr}\delta r^2 + N_{\delta u}\delta\Delta u + N_{\delta uu}\delta\Delta u^2 + N_{\delta\delta\delta u}\delta^3\Delta u + N_{v\delta}vr\delta$$

Where $\Delta u = u - U$ is the disturbance in surge velocity, where X_* Y_* N_* are the reference steady-state value of X Y and N .

4. Captive model tests.

Captive model tests are of two types i.e. static tests and dynamic tests. In the static tests, a model is towed at a constant speed in the tank. It includes static drift test, static rudder test, and rudder drift test, in this study we are only considering the first two. Dynamic tests include the pure sway and yaw test, yaw drift, and yaw rudder tests are not included in this paper. These all tests are performed using a mechanism called the Planner motion mechanism. The basic equations of the Planner motion mechanisms are

$$x_E = U_c t$$

$$y_E = -y_{max} \sin \omega t$$

$$\psi = -\arctan(\varepsilon \cos \omega t) + \beta$$

Where U_c is the towing speed, y_{max} is the max amplitude, and ε is the maximum tangent of model trajectory defined as

$$\varepsilon = \frac{y_{max} \omega}{U_c}$$

The x_E corresponds to the straight motion with speed U_c in the longitudinal direction, the y_E is the sinusoidal motion with an amplitude y_{max} and frequency ω . Where ψ is a combination of sinusoidal yaw motion with drift angle β . For static drift test y_{max} , ε and ω are zero with a fixed rudder angle usually zero, this also holds for a static rudder test with a variable rudder angle in this case. For pure sway test y_{max} and ω are non-zero but ψ is zero which results in a constantly changing drift angle β . For pure yaw test y_{max} and ω are non-zero but β is zero so the model is always tangential to the path line.

5. Numerical Modelling.

5.1. Computational method.

To perform virtual captive model tests, the commercial CFD-based software STARCCM+ is used. This software solves the conservation of mass momentum and energy for both compressible and incompressible as well as steady and unsteady flows. The incompressible unsteady flow was solved by STARCCM+ by implementing the RANS equation.

The motion of the ship was coupled with fluid using dynamic fluid body interaction (DFBI). The effect of the motion of the ship on a fluid is accounted for by moving the entire fluid mesh rigidly. This technique is known as the mesh motion technique, it updates the position of the computational domain as the solver runs. A Planner motion carriage body motion option was opted inside the DFBI motions to prescribe the motion of the ship in the x-y plane in the form of sinusoidal motion. Velocity, frequency, maximum amplitude, and drift angle was specified as an input, Table 2 and 3 shows the computational cases for static and dynamic tests. [5]. For the static drift test, the max amplitude and the frequency were kept as zero, and the frequency for dynamic test models was taken as $0.075s^{-1}$ [11].

Table 2: Computational cases for static tests.

Test	Fr	β (°)	δ (°)
Static drift	0.26	0, ±0.5, ±1, ±2, ±4, ±8	0
Static rudder	0.26	0	0, ±10, ±20, ±25, ±30, ±35

Source: Authors.

Table 3: Computational cases for dynamic tests.

Test	Fr	β (°)	δ (°)	V'_{max}	r'_{max}
Pure sway	0.26	0	0	0.035	0
Pure yaw	0.26	0	0	0.051	0

Source: Authors.

VOF model was used with a High-resolution interface capturing scheme (HRIC) to capture the free surface. A finite volume discretization scheme was applied to discretize the domain into number control volumes. A segregated flow solver with a SIMPLE pressure velocity coupling scheme was used to solve the conservation equations. Pressure and velocity gradients near the walls are solved using an all y+ treatment, this treatment uses the blended wall function and can be used for a wide range of near-wall mesh densities.

5.2. Mesh generation.

The hexahedral mesh was generated using the trimmed cell mesher, the reason for using trimmed cell mesher is that it predominantly creates the hexahedral mesh with minimal skewness. Estimated Hull performance module was used to generate the mesh, it automatically generates the mesh with volumetric

refinements around the hull and at the free surface. The location and size of the vessel are based on the best practices to ensure a high-level accuracy in the solution with a minimal cell count. The mesh sensitivity of the estimated hull performance was tested by picking up one condition i.e. static drift case with zero drift angle, three different mesh sizes have been tested and the forces in the x and y direction and the moment around the z-axis were measured. The details of the mesh sensitivity study are shown in Table 4.

Table 4: Computational cases for dynamic tests.

Mesh Elements (M)	X'	Y'	N'	Simulation Time (Hrs)	% Difference		
					X'	Y'	N'
0.6	-1.10E-05	-6.5e-07	5.9e-05	5.13	-	-	-
1.5	-1.03E-05	-5.14E-07	5.50E-05	13	5.7	20	6.7
2.5	-1.04E-05	-5.17E-07	5.52E-05	23	0.97	0.58	0.36

Source: Authors.

Forces and moments are in non-dimensionalized form. 2.5M cells predict the results closer than 1.5M cells but the time taken for that is almost double, so for this study 1.5M cell mesh was chosen. Time step sensitivity was not performed in this study, instead, a time step automatically defined by the EHP has been used, which is

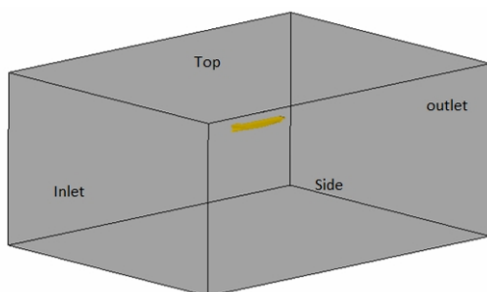
$$\text{Time step} = \text{convective time scale} / 200$$

$$\text{Convective time scale} = \text{length of ship/hull velocity}$$

5.3. Computational domain and boundary conditions.

The computational domain was made using the inbuilt estimated hull performance STARCMM+ module for marine applications. The extents of the computational domain are determined automatically and depend on the hull length between perpendiculars (Lpp). First-order VOF wave model was used to introduce the waves, wave damping was used to avoid numerical instabilities and a wave damping length was specified, EHP calculates this damping length automatically based on the Froude number and the generated computational domain. The inlet, sides, and the top of the domain were applied a velocity inlet boundary condition whereas the outlet was specified with a pressure outlet boundary condition. The hull wall was specified with a no-slip boundary condition. Fig 3 shows the computational domain and the boundary conditions.

Figure 3: Computational domain.

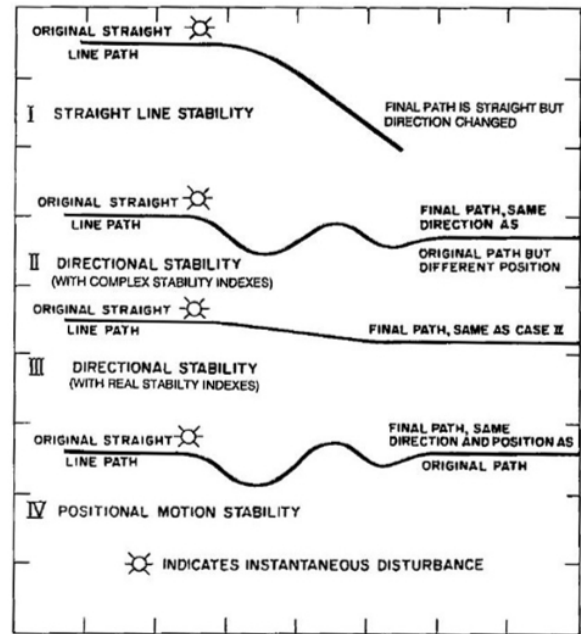


Source: Authors.

6. Results and Discussion.

Stability of ship after getting disturbed from waves or wind is of much importance, there are many types of motion stability of a ship as shown in Fig 4. A control fixed surface ship doesn't have directional stability, however, it can have straight-line stability but with working controls, a ship can achieve directional stability.

Figure 4: Motion stability kinds (PNA III).



Source: Authors.

To evaluate the straight-line stability of a ship, four linear and four angular hydrodynamic derivatives must be known i.e. the $Y_r, N_r, Y_v, N_v, Y_f, N_f, Y_{\dot{v}}, N_{\dot{v}}$. To find out these derivatives, virtual captive model tests on a benchmark KCS hull were performed additionally N_{δ} and Y_{δ} were also computed using the static rudder test. Y_v, N_v Can be computed from both the static drift test and the pure sway test but the static drift test is considered more reliable as it gives values close to experimental results. Pure sway and pure yaw tests were performed to compute the angular derivatives. In each test forces in the surge and sway forces were calculated along with the moment around the Z axis, these forces and moments were non dimensionalized using the following relations.

$$X' = \frac{X}{1/2\rho U_C^2 L_{PP}^2}$$

$$Y' = \frac{Y}{1/2\rho U_C^2 L_{PP}^2}$$

$$N' = \frac{N}{1/2\rho U_C^2 L_{PP}^3}$$

These forces and moments when plotted against the sway velocity Y_v, N_v were obtained, when plotted against rudder angle

δ , N_δ and Y_δ were obtained. Fig 5 and 6 show the comparison between experimental [12] and simulated results for X' , Y' , and N' for static drift and rudder case.

Unlike static tests, dynamic tests contain a time series of these forces and moments so to obtain Y_v , N_v and Y_r , N_r through the pure sway test. The in-phase and out of phase components with the displacements were separated. The velocity V is $\pi/2$ out of phase with the displacement so the Force and moment that were $\pi/2$ out of phase with the displacement were used to calculate Y_v and N_v , similarly, the acceleration is in phase with the displacement, so the forces and moment that were in phase with the displacements were used to compute the Y_v , N_v . Fig 7 shows the comparison between experimental and theoretical time series of X' , Y' , and N' .

Now to determine, Y_r , N_r and Y_r , N_r through pure yaw test, the same technique [13] is applied and the components in and out of phase with the yaw angle were separated and these derivatives were obtained. Fig 8 shows the time series of the non-dimensionalized forces and moments for the pure yaw case, the experimental data for the pure yaw case was not available, keeping in view the other closely predicated derivate, it was assumed to have the same accuracy. Table 5 shows the comparison between the computed derivatives and the experimental obtained derivatives.

Table 5: Comparison between simulated and experimental values.

Derivatives	Simulated values	Experimental Values	Difference (%)
Y_v	0.000215	0.000231	6.712
N_v	9.70929E-05	9.16309E-05	-5.96
Y_r	0.000483948	-	-
N_r	-0.00163	-	-
Y_δ	0.000276	0.000241157	-12.74
N_δ	0.0002	0.00021763	8.09
Y_r	9.52635E-05	-	-
N_r	-0.00022	-	-
N_δ	-1.946E-05	-2.03599E-05	4.43
Y_δ	4.2174E-05	4.22828E-05	-5.16

Source: Authors.

After obtaining all the above derivatives, the straight-line stability condition of the ship was evaluated, which is as follows. Which shows the ship possesses straight-line stability.

$$\frac{N'_r}{Y'_r+m'_\Delta} - \frac{N'_v}{Y'_v} > 0$$

Conclusions.

This paper shows the method to conduct virtual captive model tests. Hydrodynamic derivatives were evaluated by performing different captive model tests, the Experimental and theoretical results show a good comparison. The difference between experimental and theoretical results can be more improved by performing time step sensitivity study. This paper concludes that

the straight-line stability of the ship can be predicted in 5 days by using a 20 core CPU with a base speed of 2.9 GHz.

References.

ITTC, Maneuvering Committee. (2008, September). Final report and recommendations to the 25th ITTC. Proceedings of 25th International Towing Tank Conference, Fukuoka, Japan.

Zhang, S., Zhang, B., Tezdogan, T., Xu, L., & Lai, Y. (2018). Computational fluid dynamics-based hull form optimization using approximation method. *Engineering Applications of Computational Fluid Mechanics*, 12(1), 74–88. doi:10.1080/19942060.2017.1343751

Dubbioso, G., Durante, D., Di Mascio, A., & Broglia, R. (2016). Turning ability analysis of a fully appended twin-screw vessel by CFD. Part II: Single vs. Twin rudder configuration. *ocean engineering*, 117, 259–271

Abkowitz, M. A. (1964). *Lectures on ship hydrodynamics steering and maneuverability*. Lyngby: Hydro- and Aerodynamics Lab.

Simman. (2008). Workshop on verification and validation of ship maneuvering simulation methods, Copenhagen, Denmark. Retrieved from <http://www.simman2008.dk/>

Simman. (2014). Workshop on verification and validation of ship maneuvering simulation methods, Copenhagen, Denmark. Retrieved from <http://www.simman2014.dk/>

Shi He, Paula KELLETT, Zhiming YUAN, Atilla INCECIK, Osman TURAN. (2016). Maneuvering prediction based on CFD generated derivatives* DOI: 10.1016/S1001-6058(16)60630-3

Sakamoto, N., Carrica, P. M., & Stern, F. (2012). URANS simulations of static and dynamic maneuvering for surface combatant: Part 1. Verification and validation for forces, moment, and hydrodynamic derivatives. *Journal of Marine Science and Technology*, 17(4), 422–445.

Yasukawa, H., & Yoshimura, Y. (2015). Introduction of MMG standard method for ship maneuvering predictions. *Journal of Marine Science and Technology*, 20(1), 37–52. doi:10.1007/s00773-014-0293-y

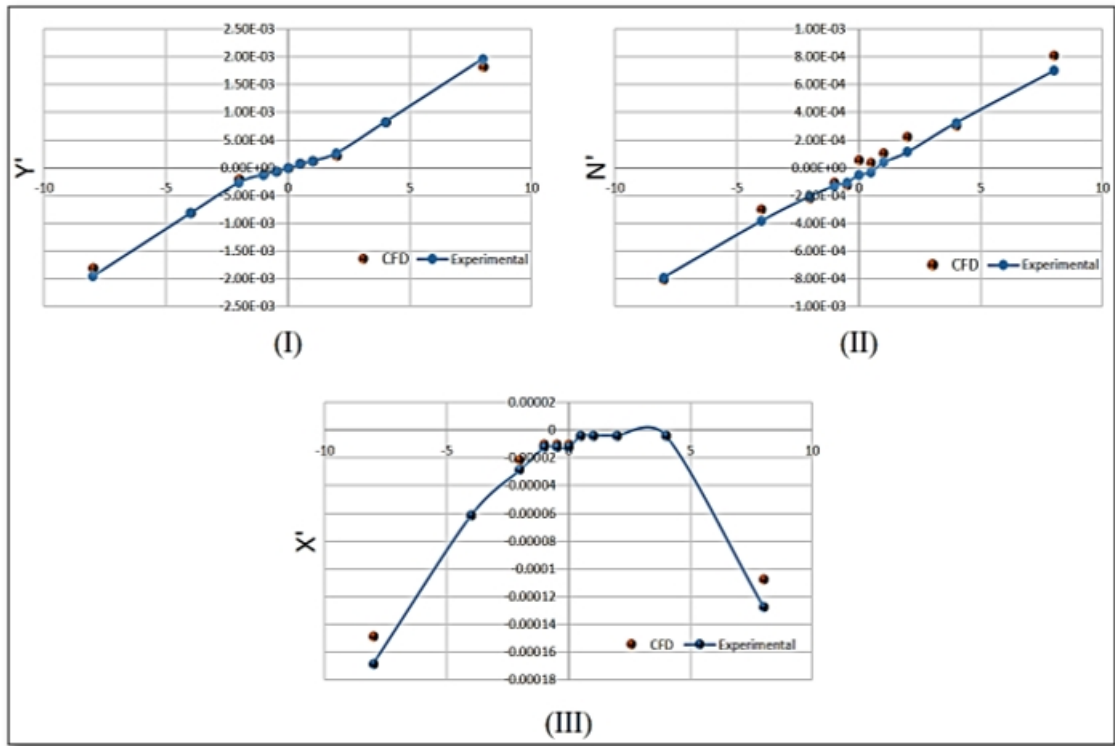
Strøm-Tejsen, J., & Chislett, M. S. (1966). A model testing technique and method of analysis for the prediction of steering and maneuvering qualities of surface vessels. Lyngby: Hydro- and Aerodynamics Lab.

Yi Liu, Lu Zou, Zaojian Zou & Haipeng Guo (2018) Predictions of ship maneuverability based on virtual captive model tests, *Engineering Applications of Computational Fluid Mechanics*, 12:1, 334-353, DOI: 10.1080/19942060.2018.1439773.

Simonsen, C.D. (2014, December). KCS PMM tests with appended hull, FORCE 2009-SIMMAN 2014. Proceedings of Workshop on Verification and Validation of Ship Maneuvering Simulation Methods, Copenhagen, Denmark.

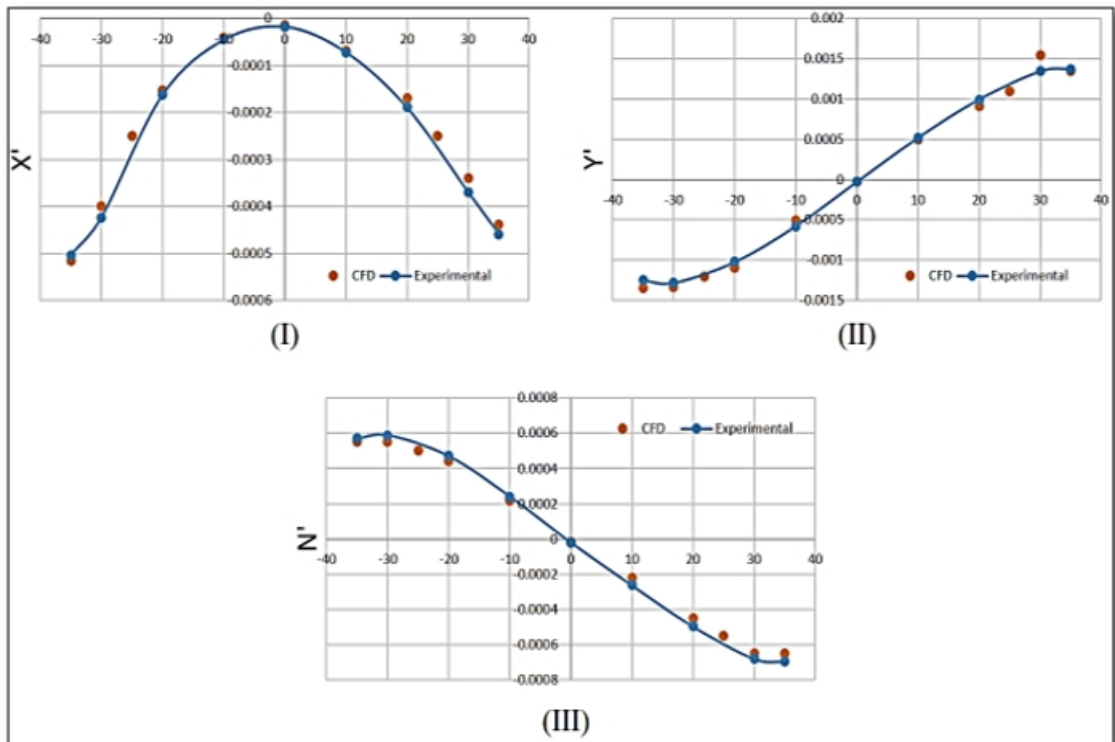
Olivier Saout (2003) computation of hydrodynamic coefficients and determination of dynamic stability characteristics of an underwater vehicle including free surface effects.

Figure 5: Static drift test results (I) Y' (II) N' (III) X' .



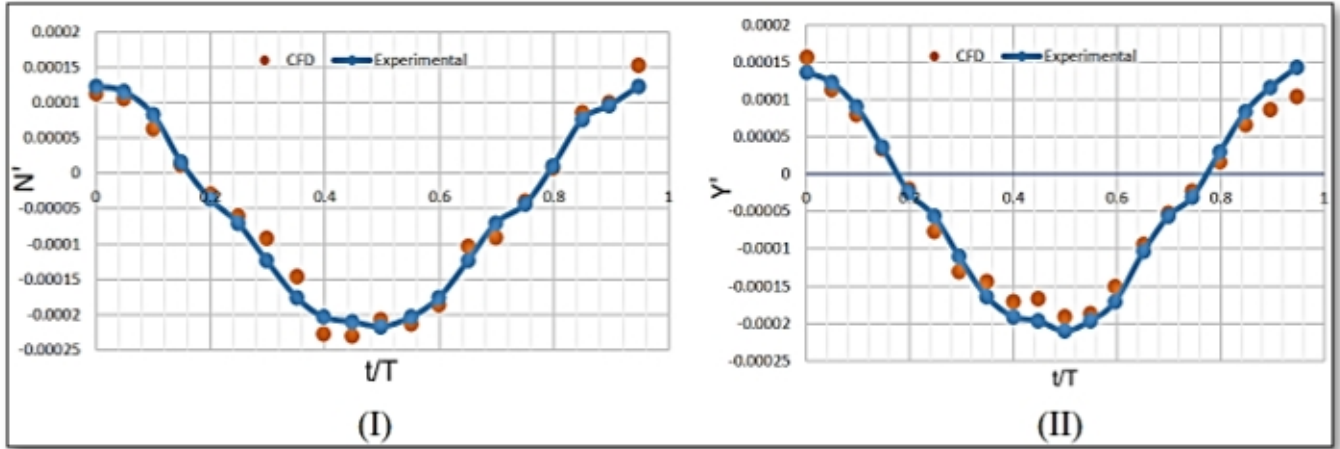
Source: Authors.

Figure 6: Static rudder test results (I) X' (II) Y' (III) N' .



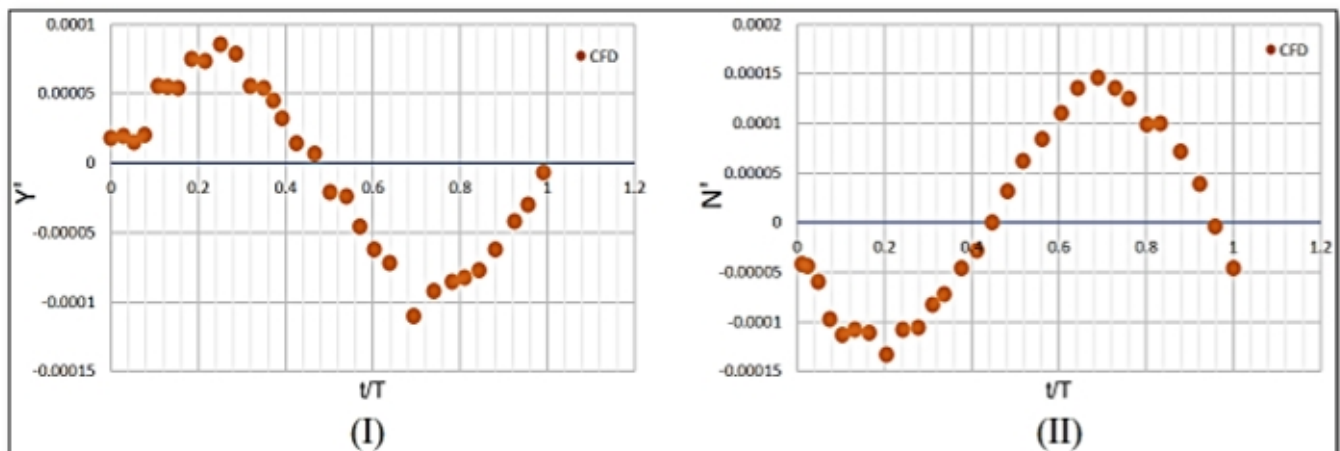
Source: Authors.

Figure 7: Pure sway test results (I) N' (II) Y' .



Source: Authors.

Figure 8: Pure Yaw test results (I) Y' (II) N' .



Source: Authors.